Improving hydrological modeling in NYC reservoir watersheds using remote sensing evapotranspiration and soil moisture products

Authors: Naira Chaouch[1], Nir Krakauer[1,2], Elliot Schneiderman[3], Marouane Temimi[1,2], Donald C. Pierson[3], Mark Zion[3], Adao Matonse[2]

Abstract

The main goal of this work is to demonstrate the efficacy of integrating remote sensing data to enhance the hydrology model GWLF that is employed by the New York City Department of Environmental Protection (NYCDEP) in the management of the New York City water supply reservoirs. The proposed approach consists of integrating remote sensing products in the modeling of hydrological processes to complement the used in situ streamflow and precipitation measurements. A MODIS evapotranspiration (ET) product was used to calibrate and verify GWLF in the Cannonsville watershed, one of those managed by NYCDEP. Three calibration scenarios were considered to introduce new calibration parameters, namely, soil water capacity, critical soil water content, and a potential evapotranspiration (PET) scale factor. Land Parameter Retrieval Model (LPRM) root zone soil moisture estimates and in situ streamflow measurements were used for model validation. The new calibration approaches result in better model performance in the simulation of evapotranspiration and similar performance in the prediction of streamflow. The calibration scenario that involves Priestley Taylor PET scale factor and soil water capacity showed better agreement between MODIS ET and model ET with Nash-Sutcliffe (NS) coefficients reaching 0.755 and 0.773 for the calibration and validation periods, respectively. Better agreement between microwave-based LPRM root zone soil moisture estimates and available water in the unsaturated zone within the watershed was also obtained after calibration with the MODIS ET product, with a root mean square difference equal to 0.159 (NS=0.41) compared to 0.171 (NS=0.32) under default calibration which implies a better closure of the water budget in the watershed. Applying hypothetical temperature changes of 1, 2 and 3 ^{o}C in GWLF revealed higher sensitivity under the new calibration of streamflow to climate change in comparison with the previously used calibration. These results show the great potential of integrating remote sensing data in hydrological models for more accurately predicting reservoir inflow, quality and quantity under climate variability and change scenarios, aiding in the management of the New York City municipal water supply.

I- Introduction

Accurate estimates of each process of the water cycle at the field, watershed, and regional scales is important for better managing water resources in terms of quantity and quality. The accuracy of the hydrological model simulation of these processes depends on model structure, availability and quality of input data, and selection of model parameters. Lumped models such us the

Generalized Watershed Loading Functions (GWLF) model (Haith et al., 1992) include conceptual parameters that are related to an aggregated conceptual description of the hydrological processes occurring in the basin. Distributed or semi-distributed models such as the Soil and Water Assessment Tool (SWAT) (Arnold and Fohrer, 2005) are based more on a physically based representation of the hydrological processes and their spatial variability within the watershed. In either case, model parameters that cannot be directly measured at the watershed scale are estimated through the process of model calibration.

The calibration process usually involves defining calibration criteria, selecting parameters to be calibrated, and running an optimization algorithm. Usually, lumped models are calibrated and verified through comparisons of the simulated and measured discharge at the basin outlet. But, particularly when there are many parameters that are calibrated, it is likely that many different parameter sets can give approximately the same model performance according to the selected objective function (equifinality) (Beven, 2002; Madsen, 2003; Bekele and Nicklow, 2007). The objective function using the root mean square error (RMSE) gives more emphasis on fitting peak streamflow values, while an objective function using RMSE for log-transformed streamflow highlights the model's ability to simulate low flows (Bekele and Nicklow, 2007). When evaluated by any one observed variable such as streamflow, the calibration process may thus result in considerable uncertainty as to the different hydrological process variables. Moreover, if an insufficient variety of calibration data are used, calibrated models may perform well in simulating the calibration data while poorly predicting processes that aren't calibrated or watershed response to climate variability and change. To enable effective adaptation, the hydrology models being used for scenario planning and operational management must accurately represent important hydrological processes. However, field data for assessing specific model capabilities, particularly those related to the representation of evapotranspiration, which is a key hydrological parameter in mid-latitude watersheds like the ones we are studying, are sparse.

Due to their detailed spatial and frequent temporal coverage, remote sensing hydrological data may provide important additional information for model calibration and validation. In fact, remote sensing satellites, including optical and active and passive microwave instruments, provide a wide variety of hydrological parameters such as soil moisture (Njoku et al., 2003; Owe et al., 2008), evapotranspiration (Mu et al., 2011; Vinukollu et al., 2011), vegetation maps, and land cover. The benefit of integrating remote sensing products in hydrological models has been demonstrated in several studies. Gao and al. (2010) considered a wide variety of remote sensing data in order to close the water budget in major US river basins. Land cover maps, NDVI, and surface temperature derived from optical remote sensing, Landsat, AVHRR and/or MODIS, are also widely used in the parameterization of hydrological models (Sucksdorff et al., 1991; Campo et al., 2006; Immerzeel et al., 2008). Immerzeel and co-authors used evapotranspiration data derived from MODIS data and the Surface Energy Balance Algorithm for Land (SEBAL) to calibrate the SWAT model (Immerzeel and Droogers, 2008; Immerzeel et al., 2008) and to assess water resources in drought conditions (Immerzeel et al., 2008) in southern India where streamflow data availability are limited. Campo and al. (2006) used soil moisture derived from synthetic aperture radar (SAR) data in the calibration of a distributed hydrological model.

The New York City supply system is one of the oldest major municipal water systems currently operating; its reservoirs, aqueducts and tunnels supplying over 9 million people. Climate change

is expected to impact the hydrology of the watersheds within the NYC water supply system (Blake et al., 2000; Frei et al., 2002; Burns et al., 2007; Matonse et al., 2011; Matonse et al., 2013). Earlier winter-spring peak streamflow combined with longer, hotter summers could negatively affect water quantity as well as water quality. The New York City Department of Environmental Protection (NYCDEP) uses GWLF to model hydrological processes in NYC watersheds. Currently, only streamflow observations are used to calibrate the GWLF model. While evapotranspiration (ET) represents the largest summer water flux affecting the water supply, evapotranspiration data are not currently used to calibrate the NYCDEP models because of the scarcity of *in situ* observations. Therefore, great interest was expressed in the assimilation of additional hydrological variables such as ET that can be derived from remote sensing observations.

This work proposes introducing evapotranspiration remote sensing-based products in the calibration and verification of the hydrological model GWLF. We assess the integration of these data in GWLF and its impact on the performance of the model. The use of remote sensing data together with in situ streamflow measurements for model calibration should improve the capabilities of the model to simulate hydrological processes in the watershed and in consequence water quantity and quality within the New York City water supply system. In this study, we compare the performance of the model when remote sensing products are introduced to the default configuration that is in use by NYCDEP, which only uses in situ observations for parameter calibration. We focus our assessment particularly on the Cannonsville (West Branch Delaware River) watershed.

II- Study area

.

Three systems form the NYC Water Supply: the Delaware, Catskill and Croton systems. Altogether, the NYC water supply system integrates a total of 19 interconnected reservoirs, three lakes, and aqueducts to supply more than 1 billion gallons (3.8×10^6 m^3) of drinking water per day to about 9 million people in NYC and nearby counties (NYCDEP 2006; Matonse et al., 2013). It is the largest surface water supply in the United States with no mechanical filtration (Daily and Ellison 2002). The Delaware and Catskill watersheds and reservoirs cover approximately 4100 km^2 in the Catskill Mountain region located west of the Hudson River at about 130 km northwest from NYC. The West of Hudson (WOH) systems contribute with more than 90% of all NYC water supply needs.

The Catskill Mountain region is part of the Allegheny Plateau mainly of sedimentary bedrock that rises up to about 1100 m in elevation from the Hudson River (Burns et al. 2007). About 70% (2850 square km) of the WOH area is part of the New York State Catskill Forest Preserve. The climate of this region is humid continental with temperatures across the region being highly impacted by elevation. Annual average temperatures range between 5.2 ^oC at higher elevations (Slide Mountain, 807 m elevation) and 7.5 ^oC at valley locations (Walton, 450 m elevation) (Matonse et al. 2013). Snow is a substantial component of annual precipitation in the Catskill Mountains, and snowmelt historically contributes between 24 and 30% of total annual runoff in this region (Matonse et al., 2011; Pradhanang et al., 2011). Regional hydrology in NYC WOH

watersheds is strongly influenced by snowpack and snow melt particularly during March and April (Matonse et al. 2011).

The West Branch Delaware River (WBDR) at Walton (USGS 01423000) watershed drains into Cannonsville Reservoir (figure 1), which together with the Pepacton and Neversink Reservoirs form the Delaware system. The WBDR watershed covers an area of 85,925 ha with elevations ranging from 370 to1020 m (590 m average elevation). The watershed is largely forested (80%) with some agriculture (14%), mainly dairy; though there has been very little change in land development and active agricultural activity have slightly declined over the last fifty years. Upstream of Walton the WBDR watershed contains no water diversions, transfers or flow regulation that significantly affect the inter- or intra-annual variability of the streamflow.

III- Methodology and data sets

First, the current performance of the model was assessed through the comparison of the streamflow and evapotranspiration estimated from the watershed model GWLF-VSLF calibrated according to current operating procedure with the corresponding in situ and remote sensing data. Evapotranspiration data are obtained using the MOD16 product derived from observations by MODIS in optical wavelengths (Mu et al., 2007). Secondly, a multi-objective calibration is developed using an objective function that quantifies the fit of GWLF output to remote sensing ET data as well as observed streamflow at the basin outlet. Our analysis uses 7 years of data (2005 -2011), divided into two groups. The first set involves data for the time period between January 1st 2005 and October 1st 2009 which is referred to hereafter as the calibration period. The second set corresponds to the simulation (validation) period and includes data from October 2nd 2009 to December 31st 2011.

III.1 Watershed model

Watershed hydrology modeling is based on the use of the new version of the Generalized Watershed Loading Functions (GWLF) model that applies a Variable Source Loading Function (VSLF) model (Schneiderman et al., 2007). Both GWLF and GWLF-VSLF are lumped-parameter models that simulate streamflow, nutrients and sediment loads on a watershed scale. Surface runoff is determined using the U.S. Department of Agriculture Soil Conservation Service Curve-Number method (USDA-SCS, 1972). GWLF considers the watershed as a composite of different hydrological response units depending on land uses, in each of which infiltration–excess runoff can occur. The GWLF-VSLF model considers in addition the saturation-excess runoff occurring in variable source areas where the soil is nearly or fully saturated within the watershed (Schneiderman et al., 2007). Based on land use and soil wetness, the basin is subdivided into 16 different land use areas classified into 10 wetness index classes. Detailed model descriptions can be found in Haith and Shoemaker (1987) and Haith et al. (1992) for the original version of GWLF, while the revised GWLF model (VSLF) is described in (Schneideman et al., 2002; 2007).

The hydrology modeling component of GWLF-VSLF requires daily precipitation, and minimum and maximum temperature or mean daily temperature data in addition to many parameters used for the calculation of different elements of the water budget. The actual evapotranspiration is

estimated from the potential evapotranspiration (PET) as limited by available moisture in the unsaturated zone (theta critical). PET is calculated using Priestley-Taylor method (Priestley and Taylor, 1972):

$$\lambda * PET = \alpha * \Delta/\Delta+\gamma * (R_{net} - G) \quad \text{(Eq. 1)}$$

Where: λ is the latent heat of vaporization, α (PET ALPHA) is a coefficient equal to 1.26 for well watered surfaces, Δ is the slope of the saturated vapor pressure - temperature curve, γ is the psychrometric constant, R_{net} is the daily net radiation, and G is the soil heat flux and supposed equal to 0 in the GWLF model.

III.2 Remote sensing data

III.2.1 Evapotranspiration

The evapotranspiration product derived from MODIS, MOD16, data and delivered by University of Montana was considered in this study. The product is global and has 1 km^2 spatial resolution. It includes the evapotranspiration (ET), latent heat flux (LE), potential ET, potential LE and data quality flag. It is an 8-day composite product regridded to the sinusoidal projection.

MODIS evapotranspiration algorithm is based on Penman-Monteith approach (Monteith, 1964). It is based on MODIS land cover, albedo, Leaf Area Index (LAI), Fraction of Absorbed Photosynthetically Active Radiation (FPAR) and daily meteorological reanalysis data from NASA's Global Modeling and Assimilation Office (GMAO) (Mu et al., 2007; Mu et al., 2011). It includes evaporation from wet and moist soil, from rain water intercepted by the canopy, and the transpiration through stomata on plant leaves and stems occurring during both daytime and nightime. We acquired MOD16 evapotranspiration data for the eight years from 2004 to 2011. A time series of mean ET values over the watershed, excluding water-covered pixels, was extracted for this period.

III.2.2 Soil moisture

In this study, the level 3 Land Parameter Retrieval Model (LPRM) root zone soil moisture product acquired from NASA server (ftp://hydro1.sci.gsfc.nasa.gov/data/s4pa/WAOB/LPRM_AMSRE_D_RZSM3.001/) at spatial resolution 0.25° is used as an additional test of the hydrological model performance. LPRM soil moisture is derived from the Advanced Microwave Scanning Radiometer-Earth Observing System (AMSR-E) data (Owe et al., 2008) through the assimilation of the LPRM/AMSR-E surface soil moisture data into the 2-Layer Palmer Water Balance Model using a 1-dimensional, 30-member Ensemble Kalman filter. LPRM/AMSR-E surface soil moisture is based on the microwave radiative transfer model to retrieve both surface soil moisture and vegetation optical depth. The land surface temperature is derived from the AMSR-E Ka-band (36.5 GHz) data (Holmes et al., 2009). LPRM root zone soil moisture data for years 2005-2011 were processed and a time series of mean values within the basin was extracted. These time series were used to assess the previously calibrated model and the model calibrated

using the new multi-objective calibration method. Since GWLF model water quantities are expressed in term of mm of water while LPRM soil moisture corresponds to volumetric water fraction, both data are normalized between their minimum and maximum values respectively for comparison.

III.3 Multi- objective calibration

For this study two calibration methods are applied: (i) a default single-objective or streamflow based calibration, and a (ii) new multi-objective calibration.

Streamflow based calibration

Single-objective calibration of the model parameters is the default in the original GWLF model. This algorithm uses an automated stepwise approach based on Powell's optimizer method (Powell, 1964). During this calibration process, measured and simulated streamflow at the basin outlet are compared for the calibration years 2005-2009 while adjusting the following calibration parameters, which mostly affect basin runoff: precipitation correction factor, melting coefficient, minimum and maximum soil water storage (S_{min} factor and S_{max} factor), runoff recess coefficient, recess coefficient and bypass coefficient. Optimal parameter sets that minimize the sum of the squared errors between observed and simulated streamflow are selected.

Multi-objective calibration

A new multi-objective calibration method is also applied. In this new calibration, GWLF-VSLF model parameters are calibrated using MODIS evapotranspiration data in combination with observed streamflow. This method will be referred hereafter as "new calibration method". The new method applies a stepwise calibration method, default calibration parameters, and calibration criteria similar to the single-objective approach above.. However, this new calibration implies in addition the consideration of others parameters that affect the estimation of the evapotranspiration and are not taken in consideration in the default calibration. . The multi–objective calibration comprises optimization of objective functions that compare both streamflow and evapotranspiration data with corresponding simulated variables for the same calibration years 2005-2009.

Selected model calibration parameters represent those to which modeled evapotranspiration is most sensitive, according to an initial model parameter sensitivity analysis. This sensitivity analysis revealed three parameters as important in GWLF-VSLF model structure and its evapotranspiration module (figure 2 and Eq.1): 1- soil water capacity (SWC); 2- critical soil water content (theta critical) and 3- Priestley Taylor constant (PET ALPHA). The soil water capacity corresponds to the field capacity of the unsaturated zone of the soil and the default value is taken equal to 10.83 cm which corresponds to the weighted average value of all land uses and soils in the watershed. The critical soil water content (theta critical) corresponds to the fraction of total available soil water between the field capacity (1) and the wilting point (0) that is readily available for transpiration. Typical values of theta critical are between 0.5 and 0.8 (Maidment Handbook of hydrology, 1993). This parameter has the default value of 0.5. The Priestley Taylor

constant (PET ALPHA) parameterizes the resistance to evaporation and it is equal to 1.26 for wet and humid conditions. The GWLF-VSLF model considers a default value of 1.28 for PET ALPHA.

Three calibration scenarios were defined to assess the integration of the MOD16 remote sensing product in the calibration process of the model. The first scenario (CAL1) considers the PET ALPHA to match daily model-simulated and MOD16 evapotranspiration data. The second scenario (CAL2) corresponds to the calibration of both PET ALPHA and soil water capacity. The third scenario (CAL3) considers in addition the theta critical parameter. All these calibration scenarios have the objective of matching daily model evapotranspiration and MODIS evapotranspiration along with minimizing the discrepancies between observed and estimated discharge.

III.4 Validation

The results of the new calibration method are evaluated using observed streamflow discharge at the outlet of the WBDR basin for the period 2010 and 2011, basin-averaged MODIS evapotranspiration, and LPRM root zone soil moisture for the same time period. The performance of the calibrated models is evaluated using the Nash-Sutcliffe efficiency coefficient (NS) and Root Mean Square Error (RMSE):

$$NS= 1- \sum(M_i-O_i)^2/\sum(O_i-\text{mean}(O_i))^2$$

$$RMSE= (1/N * \sum(O_i- M_i)^2)^{1/2}$$

where: M_i is the modeled, and O_i is the observed value at the time i, and N is the total number of observations.

IV- Results

The daily analysis of the simulated streamflow and in situ measurements shows a good agreement between both sources with a NS coefficient equal to 0.79, figure 3-a. Recall that the calibration of the model intends to minimize the mean squared difference between modeled and in situ streamflow. It is worth noting that the default calibration aims also to close total streamflow budget for the calibration period between January 2005 and October 2009. When the total budget is considered for the simulation period, the model tends to overestimate the streamflow (figure 3-b) which may affect the water partition between different processes of the water budget. In fact, for the same precipitation amount, an overestimation of the streamflow can be due to an underestimation of either evapotranspiration or storage. Moreover, a good agreement between simulated and in situ streamflow does not always reflect a good estimation of other components of the water budget (e.g. storage and evapotranspiration).

Figure 4-a shows that the pre-calibrated model underestimates the evapotranspiration with respect to MODIS evapotranspiration values especially during winter time and under dry summer conditions (July 2005, summer 2007, June 2010). The comparison of the model evapotranspiration with MODIS evapotranspiration shows an underestimation of the total model ET budget, figure 4b. During winter, model ET is always less than MODIS ET and it is usually equal to zero, figure 5. It is worth noting that the model actual evapotranspiration is estimated using potential evapotranspiration (PET) determined using Priestley-Taylor method which is based on the net radiation and temperature. Daily net radiation is often negative in winter, which leads to an estimated Priestley-Taylor PET equal to zero. However, actual evapotranspiration is positive in MOD16 because of daytime net radiation. This finding is in line with previous work by Van Kraalingen and Stol (1997) which showed that Priestley-Taylor method could not be applied to estimate winter ET for the Netherlands. Also, Irmak and al. (2003) found that Priestley-Taylor method underestimates ET in winter and overestimates it during summer months for Gainesville, Florida. Under advective conditions, Berengena and Gavilan (2005) reported an ET underestimation of 23% on average with Priestley-Taylor method. The underestimation of model ET can be explained also by the fact that GWLF model does not consider evaporation from snow surfaces and from vegetation-intercepted rainfall. For forests and on an annual basis, evaporation from intercepted water ranges between 10 and 40 % of the total precipitation depending on the canopy's structure, rainfall intensity and climates (Rutter and A.J., 1977; Gash et al., 1980; Shuttleworth, 1988; Crockford and Richardson, 2000; Miralles et al., 2011) .

In early spring, the model overestimates evapotranspiration in comparison with MODIS ET, figure 5. This fast model spring increase in ET may be partly due to the shutdown of the evapotranspiration process during the winter time, leaving more water available to evaporate in early spring. But, the greater evapotranspiration modeled during this period results on a decrease of the water availability in the soil for eventual evaporation later during summer. This is observed especially during summers 2005 and 2007 with an early depletion of model ET. Moreover, an underestimation of the evapotranspiration results in seasonal overestimation of the streamflow and vice versa (figures 3-a, 4-a and table 1). ET underestimation is more noticeable under dry conditions and low precipitation amounts. In late summer 2005 for example, the model overestimates streamflow in comparison with in situ measurements while it underestimates ET compared to MOD16 (from 07/20/2005 to 10/31/2005, ET model=161.8 mm, MODIS ET = 285.05 mm, Q model= 75.72 mm and Q in situ= 59.51 mm).

The analysis of modeled PET variation (figure 6) during these three summer seasons showed high PET values while actual ET does not reach the PET. Thus, the underestimation of the summer ET results from land surface controls and not from the available energy (PET). In order to improve the evapotranspiration estimation, it is then necessary to calibrate the important model parameters having control over the evapotranspiration calculation.
In GWLF model (figure1), the estimation of the evapotranspiration depends among others on the soil water capacity (soil water cap), critical soil content (theta crit) and the Priestley Taylor potential evapotranspiration constant (PET ALPHA, Eq.1). These parameters are not calibrated in the default version of the GWLF-VSLF model. Their values are defined from the literature, while here we consider an acceptable range of values, with the actual value to be used to be determined by calibration. Different values can lead to different model behaviors. For a

sensitivity analysis, different simulations were carried out using different values of soil water capacity (15, 20, 30 cm), theta critical (0.2, 0.6 and 0.8) and PET ALPHA (0.7 and 1) in addition to the default values used in the pre-calibrated model. Figure 7 presents time series variation of the model evapotranspiration considering these different scenarios. An increase in soil water capacity leads to an increase of modeled ET especially for summers 2005, 2007, 2008 and 2010 where it showed early depletion in GWLF in comparison with MODIS ET, figure 7-a. This can be explained by the fact that the increase of soil water capacity results in an increase of the amount of water stored in the unsaturated zone and available for evapotranspiration. Considering summer periods, the increase (177.8 %) of SWC from 10.8 cm (default value) to 30 cm results in an increase of total evapotranspiration of 7.1 % and a decrease of streamflow by 4.3%. For the time period between January 2005 and December 2011, better agreement between simulated evapotranspiration and MODIS ET is obtained with NS equal to 0.73 for SWC equal to 30 cm while it is equal to 0.68 at the default parameter value. Figure 7-b shows high ET sensitivity to PET ALPHA. Recall that a decrease of PET ALPHA results in a decrease of the potential evapotranspiration values and in consequence of the actual evapotranspiration values. A decrease (45%) of PET Alpha from 1.28 (default value) to 0.7 led to a decrease of simulated ET total budget by 41.1% and an increase of simulated streamflow total budget by 25.1%. Figure 7-c demonstrates a decrease of simulated ET in function of theta-critical values. This decrease results from the soil resistance to evaporation because of soil moisture constraint. An increase of theta critical from 0.2 to 0.8 led to a decrease of 7.6 % of the total evapotranspiration and an increase of 4.6 % of the total streamflow. These results illustrate the importance of these parameters in ET simulation and suggest the need of their calibration to MODIS ET variation in order to improve model ET estimates especially for spring and summer periods.

The multi-objective calibration method led to an improvement of evapotranspiration (figure 8-b) and streamflow (figure 8-a) estimates, although improvement was less significant in the case of the latter (table 2). Different PET ALPHA, soil water capacity and theta critical values are obtained considering the three new calibration scenarios, table 3. Calibration scenario Cal1 results on PET ALPHA value (1.11) less than the default one (1.28). This scenario remediates the overestimation of model ET in comparison with MODIS ET observed early spring but results on further reduction of model ET during the summer, figure 8-b. For the latter period, an increase of the soil water capacity as obtained by the calibration scenario Cal2 results on better agreement between both ET data with NS values equal to 0.755 and 0.773 for the calibration and simulation periods, respectively. Calibration scenario 3 (Cal3) did not show additional improvement of ET estimates compared to the other scenarios and particularly with scenario 2. It results on soil water capacity (29.99 cm) and PET ALPHA (1.11) values identical as Cal2 while the optimized theta critical showed insignificant change from the original value of 0.5. The calibration of the GWLF model using MODIS ET results on an increase of soil water capacity and a decrease of PET ALPHA when compared to the default calibration. Previous studies showed that the value of PET ALPHA is related to soil moisture (Flint and Childs, 1991; Fisher et al., 2005), air temperature (Berengena and Gavilan, 2005) and show seasonal variation. For water stressed surfaces, it decreases from its default value defined for ultimate conditions (Stannard, 1993). For semiarid regions and under advective conditions, Berengena and Gavilan (2005) suggests the need to adjust PET ALPHA in function of wind speed, temperature and vapor pressure. For better evapotranspiration estimates, it is then necessary to calibrate PET ALPHA factor on a regional scale under different climates.

Moreover, since these calibration scenarios result on an overall increase of evapotranspiration and decrease of streamflow, they consequently affect water partition between different components of the water budget like the water availability within the unsaturated zone. Figure 9 shows time variability of the quantity of water available in the unsaturated zone within the watershed and the LPRM root zone soil moisture, which was not used in the calibrations. Better agreement between both data are obtained with root mean square difference equal to 0.148 (NS=0.49) and 0.159 (NS=0.41) considering Cal 1 and Cal 2, respectively. A root mean square error equal to 0.171 (NS=0.32) is obtained using default calibration parameters.

For winter time, these parameters do not show a significant impact on the estimated evapotranspiration values. The underestimation of the ET in winter can be explained by the fact that Priestley Taylor method is based on the daily net radiation which is negative during this time of the year. In addition, GWLF does not describe the evapotranspiration occurring from intercepted rainfall water in the vegetation and from snow sublimation. Since our priority for water quantity and quality applications is summer drought and low streamflow conditions, we do not attempt to modify GWLF in this study to represent snow sublimation and interception, but these processes should be considered in future work. Moreover, the fact of using daily values of the temperature, humidity and net radiation to calculate the Priestley-Taylor potential evapotranspiration can lead to significant errors. Since net radiation is positive during the daytime and negative during nighttime, better evapotranspiration estimation may be obtained when it is calculated on an hourly basis. In fact, daily evapotranspiration calculation using daytime and nighttime Priestley Taylor potential evapotranspiration results in better agreement between simulated and MODIS ET, table 2. Higher NS coefficients between MODIS ET and model ET are obtained considering the same three calibration scenarios but calculating actual evapotranspiration from daytime and nighttime potential evapotranspiration (CalDN1, CalDN2, and CalDN3).

Previous work on New York City's water supply system showed that future changes in temperature and precipitation will affect evapotranspiration rate and water availability (Blake et al., 2000; Frei et al., 2002) and consequently will lead to changes in each component of the water budget. Table 4 presents the sensitivity of the GWLF-VSLF model with the default calibration and new calibrations (Cal1, Cal2) and also the new GWLF version considering daytime and nighttime potential evapotranspiration for the calculation of actual evapotranspiration (CalDN1, CalDN2) to hypothetical uniform warming of the observed temperature time series by 1 ^{o}C, 2 ^{o}C, or 3^{o}C. The new calibrations (especially Cal2) and versions of GWLF model tend to show more sensitivity of streamflow to temperature change. Table 4 shows that the increase of temperature led to an increase of total evapotranspiration budget and a decrease of the total streamflow budget over the study period. Using the GWLF with the new calibrated parameters, for each uniform 1 ^{o}C increase of the temperature an increase of the total ET of 2.4 - 3.3% and a decrease of the total streamflow by 1.4 - 2.1% are obtained. The original calibrated model shows a smaller ET increase by 2.1 - 2.4% and a decrease of 1.4 - 1.5% in streamflow for each 1^{o}C temperature increase. These preliminary results illustrate the importance of an accurate hydrological model parameterization and calibration for a reliable prediction of the water supply in New York City in climate change perspective.

V- Conclusions

The comparison of GWLF-VSLF modeled evapotranspiration and MODIS evapotranspiration data indicated large discrepancies between the two time series especially during early spring, winter, and dry late summers. GWLF-VSLF as calibrated using only streamflow *in situ* measurements may lead to errors in the closure of the water budget in the model.

A multi calibration method using remote sensing evapotranspiration in addition to in situ streamflow data was applied for better model calibration. The most important parameters affecting the calculation of the evapotranspiration were calibrated using a remote sensing based ET product. This results on better agreement between simulated and MODIS ET and also slightl improvement of the estimated streamflow especially during summer time. For the winter, Priestley-Taylor method predicts PET equal to zero while actual evapotranspiration is positive. Modifications to the model structure may be necessary for potential evapotranspiration estimation during winter months.

The new calibrated model showed better water partition between the different water processes as measured by agreement with streamflow and ET data for the validation period, and better agreement with the LPRM soil moisture product was also obtained. These results show the importance of considering different sources of information, not just streamflow, to validate and calibrate watershed models for accurate estimation of the water supply especially under dry conditions.

Applying a hypothetical warming of 1, 2 and 3 ^{o}C showed more sensitivity of the new calibrated model to the change in temperature. Under these scenarios, water yields are projected to be lower using the new calibrated model. Accurate model parameterization and good estimates of model parameters related to ET are necessary for better estimates of the water supply within the watershed for operational management or future scenarios analysis.

This work showed the benefit of the use of remote sensing data for model validation and calibration for municipal water supply management and planning applications. Our results illustrate the potential of the integration of the remote sensing data into the hydrological model for better partition between different water processes within the water budget. Other remote sensing data, like soil moisture and snow properties, could be also assimilated into the GWLF model. This will be addressed in future study.

References

Arnold, J. G. and N. Fohrer (2005). "SWAT2000:Current capabilities and research opportunities in applied watershed modeling." Hydrological Processes **19**(13): 563-572.

Bekele, E. G. and J. W. Nicklow (2007). "Multi-objective automatic calibration of SWAT using NSGA-II." Journal of Hydrology **341**(3-4): 165-176.

Berengena, J. and P. Gavilan (2005). "Reference Evapotranspiration Estimation in a Highly Advective Semiarid Environment." Journal of Irrigation and Drainage Engineering **131**(2): 147-163.

Beven, K. (2002). "Towards a coherent philosophy for modelling the environment." Proc. R. Soc. Lond. A **Vol. 458**(no. 2026): 2465-2484.

Blake, R., R. Khanbilvardi and C. Rosenzweig (2000). "Climate change impacts on the New York City's water supply system." Journal of the American Water Resources Association **36**: 279-292.

Burns, D. A., J. Klaus and M. R. McHale (2007). "Recent climate trends and implications for water resources in the Catskill Mountain region, New York, USA." Journal of Hydrology **336**(1-2): 155-170.

Campo, L., F. Caparrini and F. Castelli (2006). "Use of multi-platform, multi-temporal remote-sensing data for calibration of a distributed hydrological model: An application in the Arno basin, Italy." Hydrological Processes **20**(13): 2693-2712.

Crockford, R. H. and D. P. Richardson (2000). "Partitioning of rainfall into throughfall, stemflow and interception: effect of forest type, ground cover and climate." Hydrological Processes **14**(16-17): 2903-2920.

Daily GC, K Ellison. 2002. *The new economy of nature : the quest to make conservation profitable*, Island Press, Washington DC. Chapter **3**: 61-85.Fisher, J. B., T. A. Debiase, Y. Qi, M. Xu and A. H. Goldstein (2005). "Evapotranspiration models compared on a Sierra Nevada forest ecosystem." Environmental Modelling and Software **20**(6): 783-796.

Flint, A. L. and S. W. Childs (1991). "Use of the Priestley-Taylor evaporation equation for soil-water limited conditions in a small forest clear-cut." Agricultural and Forest Meteorology **56**: 247-260.

Frei, A., R. L. Armstrong, M. P. Clark and M. Serreze (2002). "Catskill Mountain Water Resources: Vulnerability, Hydroclimatology and Climate-change Sensitivity." Annals of the Association of American Geographers **92**(2): 203-224.

Gash, J. H., I. R. Wright and C. R. Lloyd (1980). " Comparative estimates of interception loss from three coniferous forests in Great Britain." Journal of Hydrology **48**: 89-105.

Haith, D. A., R. Mandel and R.S. Wu (1992). "Generalized Watershed Loading Functions Version 2.0 User's Manual, Cornell University, Ithaca, New York.".

Holmes, T. R. H., R. A. M. De Jeu, M. Owe and A. J. Dolman (2009). "Land surface temperatures from Ka-Band (37 GHz) passive microwave observations." Journal of Geophysical Research **114**(D04113).

Immerzeel, W. W. and P. Droogers (2008). "Calibration of a distributed hydrological model based on satellite evapotranspiration." Journal of Hydrology **349**(3-4): 411-424.

Immerzeel, W. W., A. Gaur and S. J. Zwart (2008). "Integrating remote sensing and a process-based hydrological model to evaluate water use and productivity in a south Indian catchment." Agricultural Water Management **95**(1): 11-24.

Irmak, S., A. Irmak, R. Allen and J. Jones (2003). "Solar and Net Radiation-Based Equations to Estimate Reference Evapotranspiration in Humid Climates " Journal of Irrigation and Drainage Engineering **129**(5): 336-347.

Madsen, H. (2003). "Parameter estimation in distributed hydrological catchment modelling using automatic calibration with multiple objectives." Advances in Water Resources **26**(2): 205-216.

Matonse, A. H., D. C. Pierson, A. Frei, M. S. Zion, A. Anandhi, E. Schneiderman and B. Wright (2013). "Investigating the impact of climate change on New York City's primary water supply." Climatic Change **116**(3-4): 437-456.

Matonse, A. H., D. C. Pierson, A. Frei, M. S. Zion, E. M. Schneiderman, A. Anandhi, R. Mukundan and S. M. Pradhanang (2011). "Effects of changes in snow pattern and the timing of runoff on NYC water supply system." Hydrological Processes **25**(21): 3278-3288.

Miralles, D. G., R. A. M. De Jeu, J. H. Gash, T. R. H. Holmes and A. J. Dolman (2011). "Magnitude and variability of land evaporation and its components at the global scale." Hydrology and Earth System Sciences **15**(3): 967-981.

Monteith, J. L. (1964). Evaporation and environment. The state and movement of water in living organisms. Symposium of the Society of experimental biology. Cambridge, Cambridge University Press. **Vol.19:** pp. 205-234.

Mu, Q., F. A. Heinsch, M. Zhao and S. W. Running (2007). "Development of a global evapotranspiration algorithm based on MODIS and global meteorology data." Remote Sensing of Environment **111**(4): 519-536.

Mu, Q., M. Zhao and S. W. Running (2011). "Improvements to a MODIS global terrestrial evapotranspiration algorithm." Remote Sensing of Environment **115**(8): 1781-1800.

Njoku, E. G., T. J. Jackson, V. Lakshmi, T. K. Chan and S. V. Nghiem (2003). "Soil moisture retrieval from AMSR-E." IEEE Transactions on Geoscience and Remote Sensing **41**(2 PART 1): 215-228.

NYCDEP. 2006. New York City Water Supply System Reference Guide, NYCDEP Bureau of Water Supply, Valhalla, New York.Owe, M., R. De Jeu and T. Holmes (2008). "Multisensor historical climatology of satellite-derived global land surface moisture." Journal of Geophysical Research **113**(F01002).

Powell, M. J. D. (1964). "An efficient method for finding the minimum of a function of several variables without calculating derivatives." Computer Journal **7**(2): 155-162.

Pradhanang, S. M., A. Anandhi, R. Mukundan, M. S. Zion, D. C. Pierson, E. M. Schneiderman, A. Matonse and A. Frei (2011). "Application of SWAT model to assess snowpack development and streamflow in the Cannonsville watershed, New York, USA." Hydrological Processes **25**(21): 3268-3277.

Priestley, C. H. B. and R. J. Taylor (1972). "On the assessment of surface heat flux and evaporation using large-scale parameters." Monthly Weather Review **100**: 81-82.

Rutter, A. J. and M. A.J. (1977). "A predictive model of rainfall interception in forests. III. Sensitivity of the model to stand parameters and meteorological variables." Journal of Applied Ecology **14**: 567-588.

Schneideman, E. M., D. C. Pierson, D. G. Lounsbury and M. S. Zion (2002). "Modeling the hydrochemistry of the cannonsville watershed with Generalized Watershed Loading Functions (GWLF)." Journal of the American Water Resources Association **38**(5): 1323-1347.

Schneiderman, E. M., T. S. Steenhuis, D. J. Thongs, Z. M. Easton, M. S. Zion, A. L. Neal, G. F. Mendoza and M. T. Walter (2007). "Incorporating variable source area hydrology into a curve-number-based watershed model." Hydrological Processes **21**(25): 3420-3430.

Shuttleworth, W. J. (1988). "Evaporation from Amazonian Rainforest." Proceedings of the Royal Society of London. Series B. Biological Sciences **233**(1272): 321-346.

Stannard, D. I. (1993). "Comparison of Penman-Monteith, Shuttleworth-Wallace, and modified Priestley-Taylor evapotranspiration models for wildland vegetation in semiarid rangeland." Water Resources Research **29**: 1379-1392.

Sucksdorff, Y., G. Michels, S. Tattari and M. Heikinheimo (1991). Operational satellite remote sensing for hydrological modelling. 1991 International Geoscience and Remote Sensing Symposium - IGARSS'91, June 3, 1991 - June 6, 1991, Espoo, Finl, Publ by IEEE.

USDA-SCS (1972). National Engineering Handbook, Natural Resources Conservation Service, U.S. Department of Agriculture.

Van Kraalingen, D. W. G. and W. Stol (1997). Evapotranspiration Modules for Crop Growth Simulation: Implementation of the Algorithms from Penman, Makkink and Priestley-Taylor, DLO Research Institute for Agrobiology and Soil Fertility.

Vinukollu, R. K., E. F. Wood, C. R. Ferguson and J. B. Fisher (2011). "Global estimates of evapotranspiration for climate studies using multi-sensor remote sensing data: Evaluation of three process-based approaches." Remote Sensing of Environment **115**(3): 801-823.

Table 1: Comparison of cumulative streamflow (Q) and evapotranspiration (ET) budgets from May 1st to October 31st with in situ measurements and MODIS data respectively

Year	Precipitation (mm)	Model ET (mm)	MODIS ET (mm)	Model Q (mm)	In situ Q (mm)
2005	566.3	441.1	526.2	128.9	131.3
2006	876.2	501.9	459.5	347.9	444.2
2007	685.0	510.9	570.2	168.8	167.6
2008	644.4	506.4	497.0	134.8	131.2
2009	843.5	487.2	470.5	319.9	340.4
2010	773.8	484.2	553.8	283.3	241.8
2011	971.0	474.6	483.1	538.2	534.1

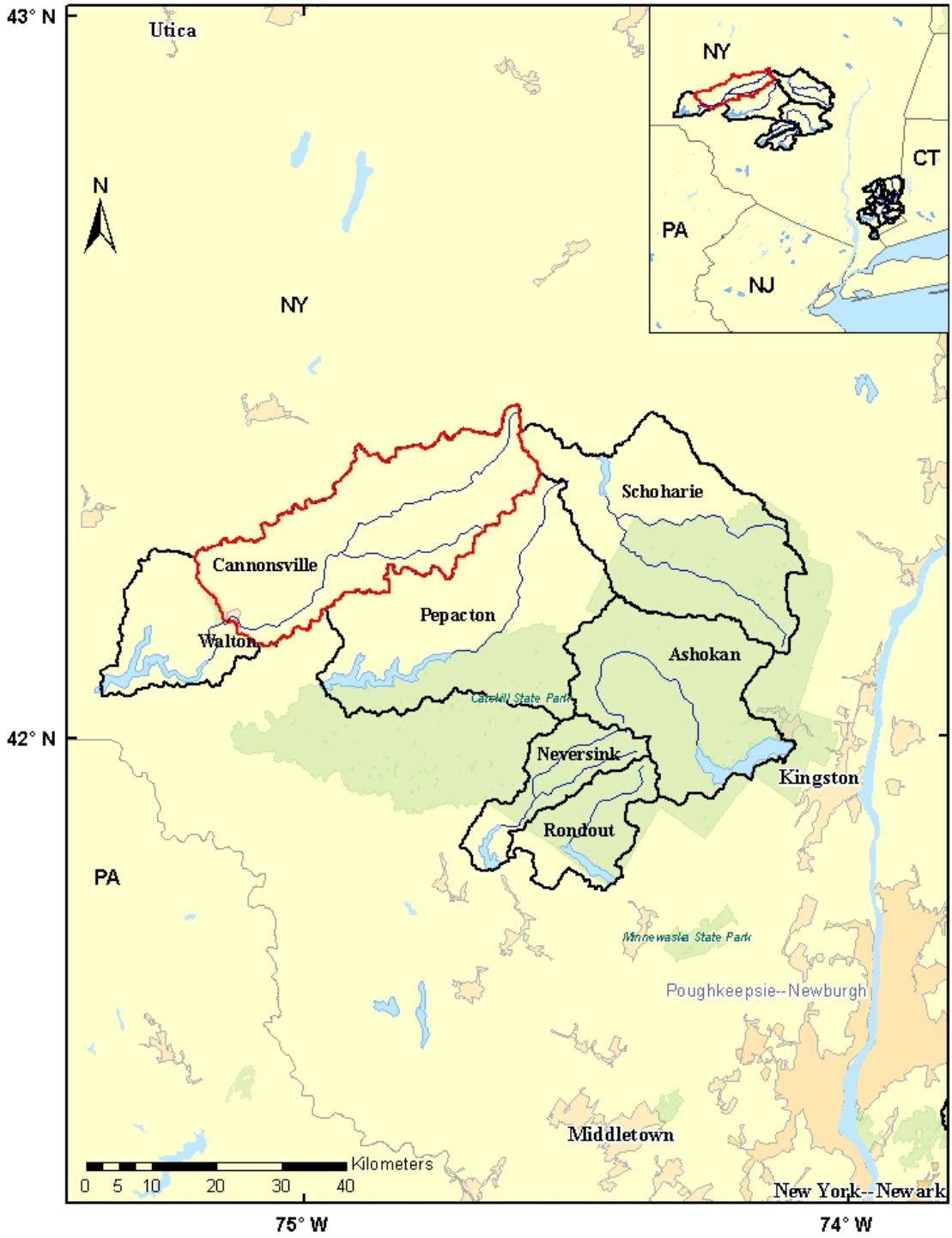

Figure 1: NYC West of the Hudson River reservoirs. The study area in this paper is the Cannonsville watershed of the West Branch Delaware River.

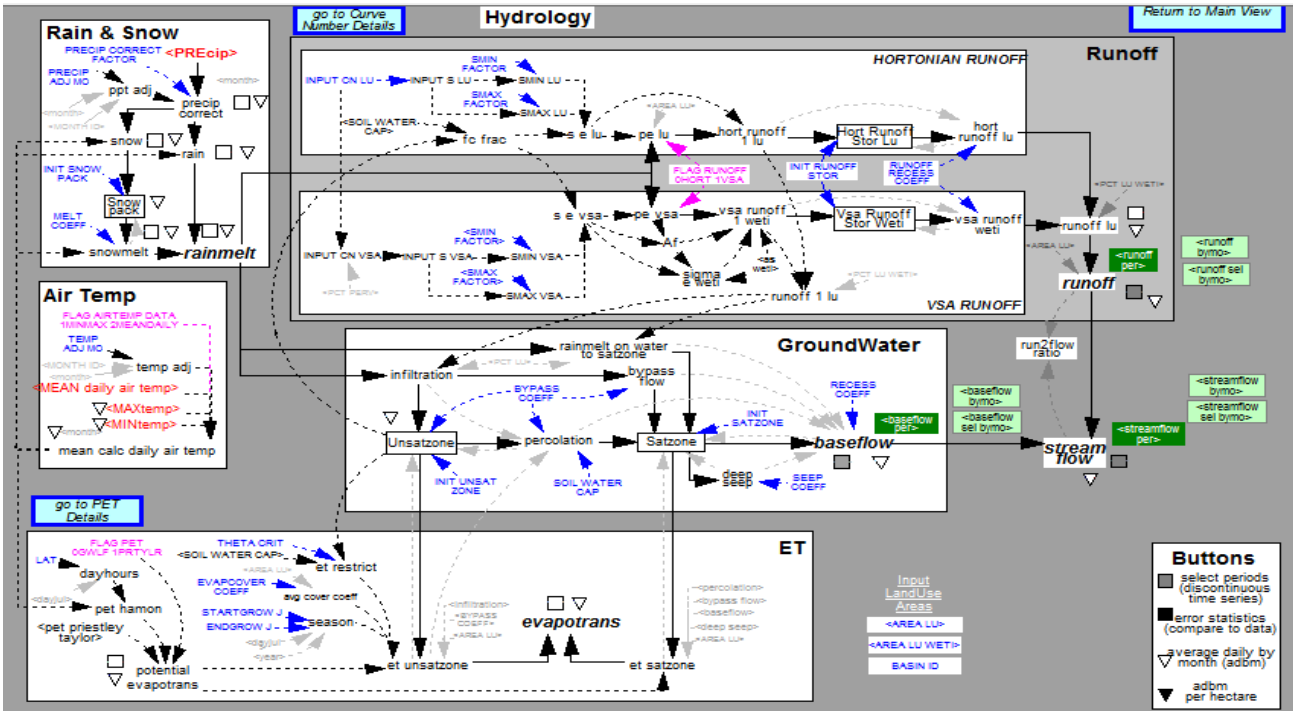

Figure 2: GWLF model parameterization and structure (Schneideman et al., 2002; Schneiderman et al., 2007)

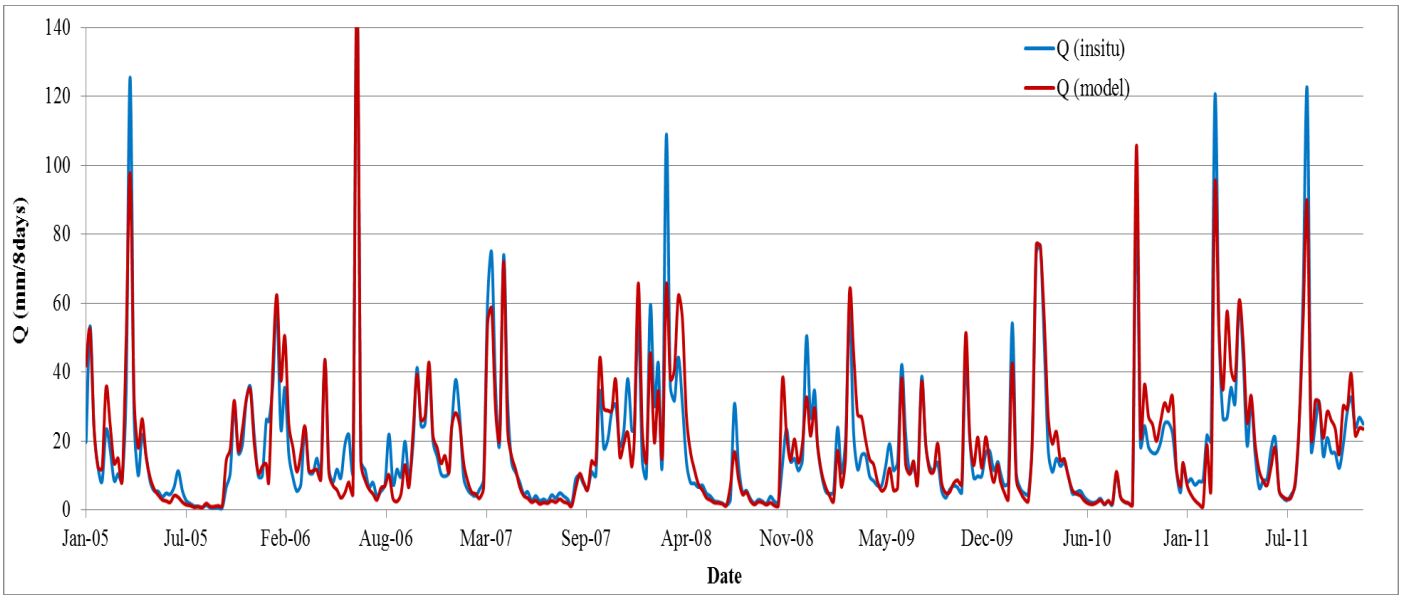

(a)

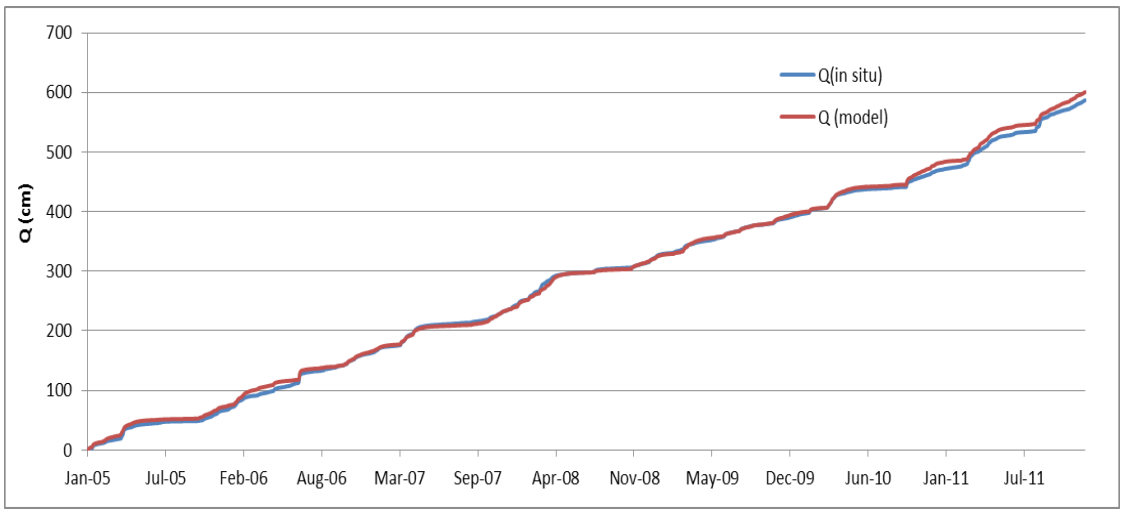

(b)

Figure 3: comparison between in situ and estimated streamflow with default parameter values for GWLF: (a): daily, (b) cumulative

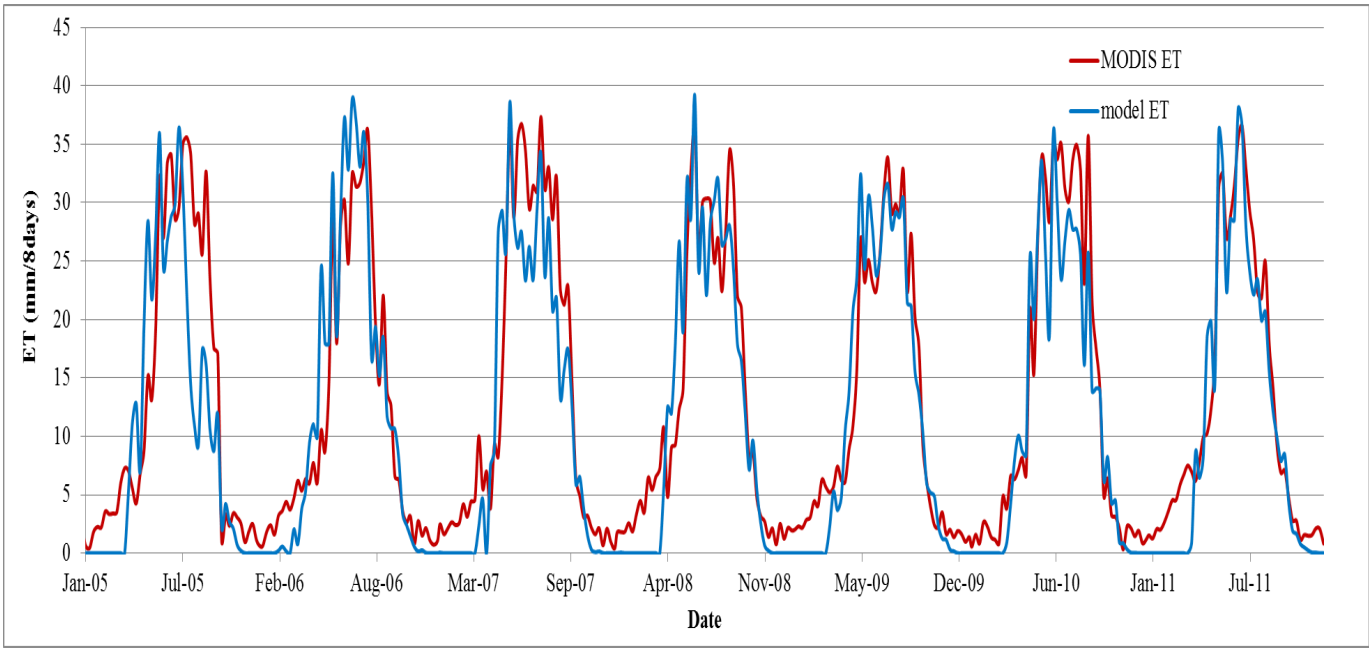

(a)

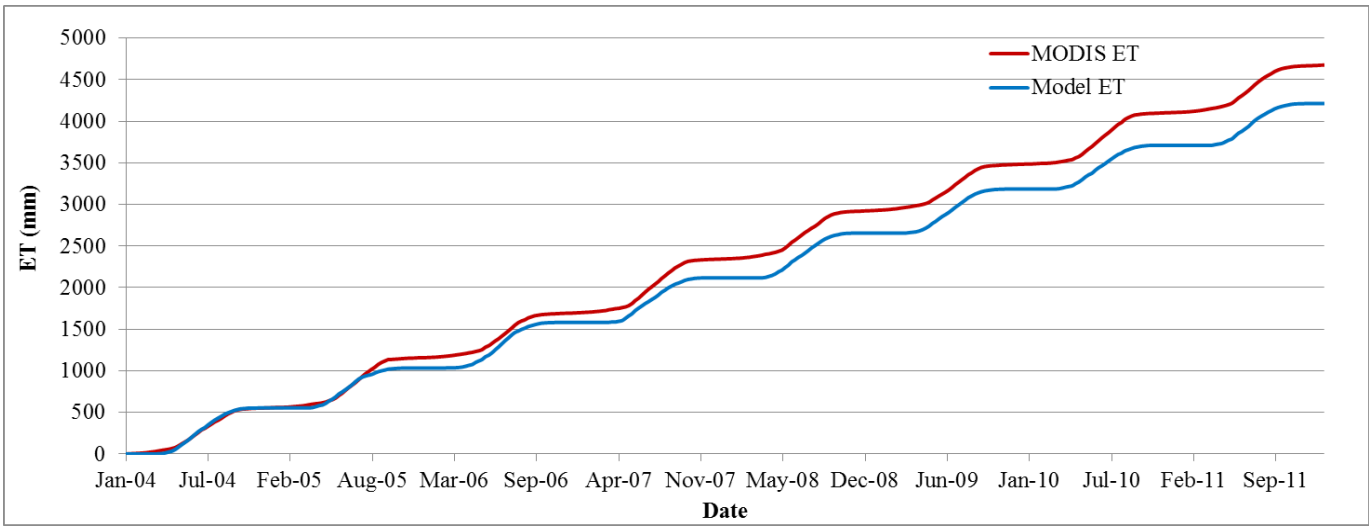

(b)

Figure 4: Comparison between model ET and MODIS ET, (a) Monthly time series, (b) cumulative budget

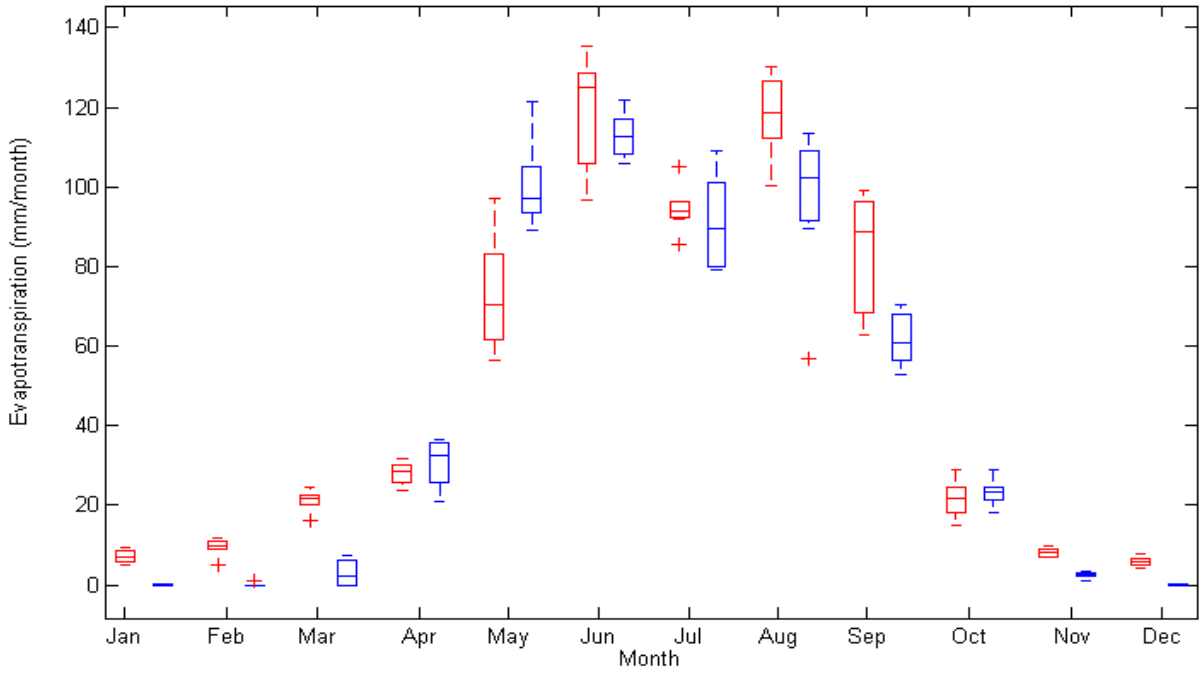

Figure 5: Monthly MODIS (red) and modeled (blue) evapotranspiration data. Box.plots represent the interquartile range for ; Whiskers represent the lowest and highest data values. horizontal lines in the box plots represent the median and '+' signs represent outliers

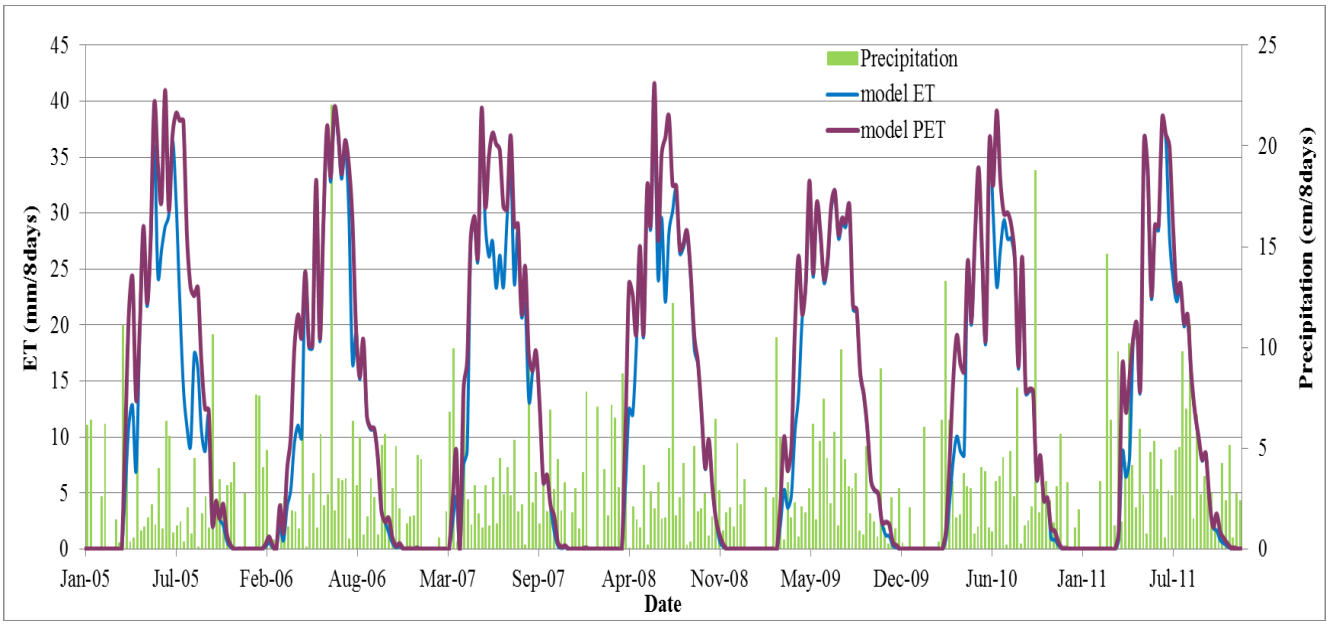

Figure 6: Simulated model ET and model PET and precipitation data

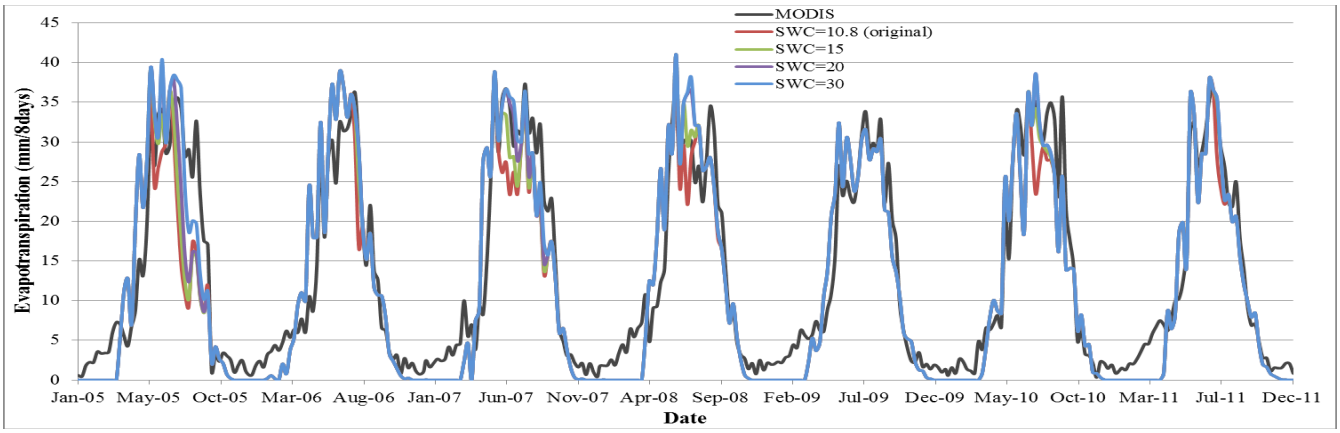

(a)

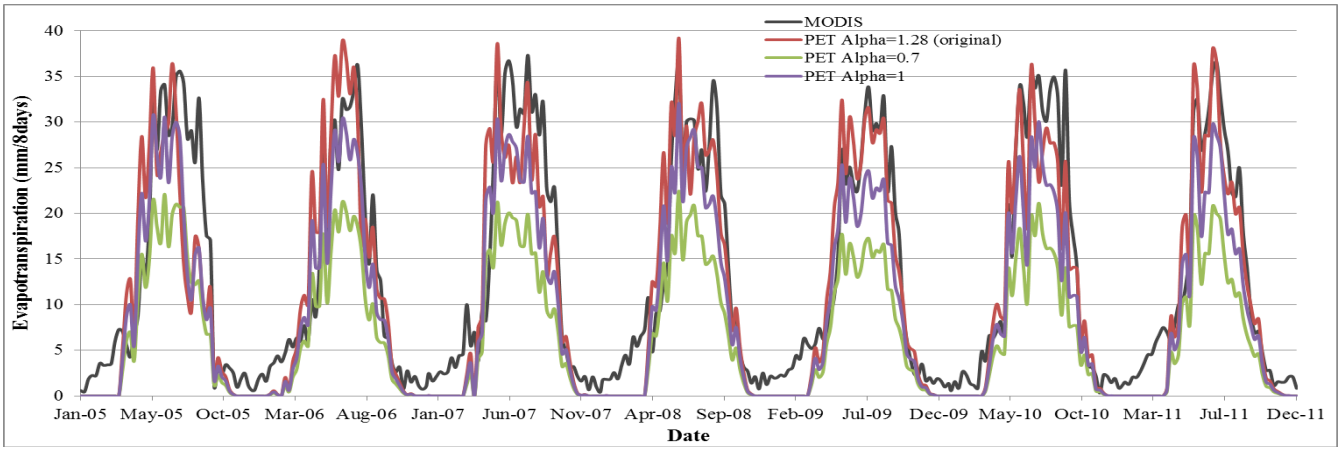

(b)

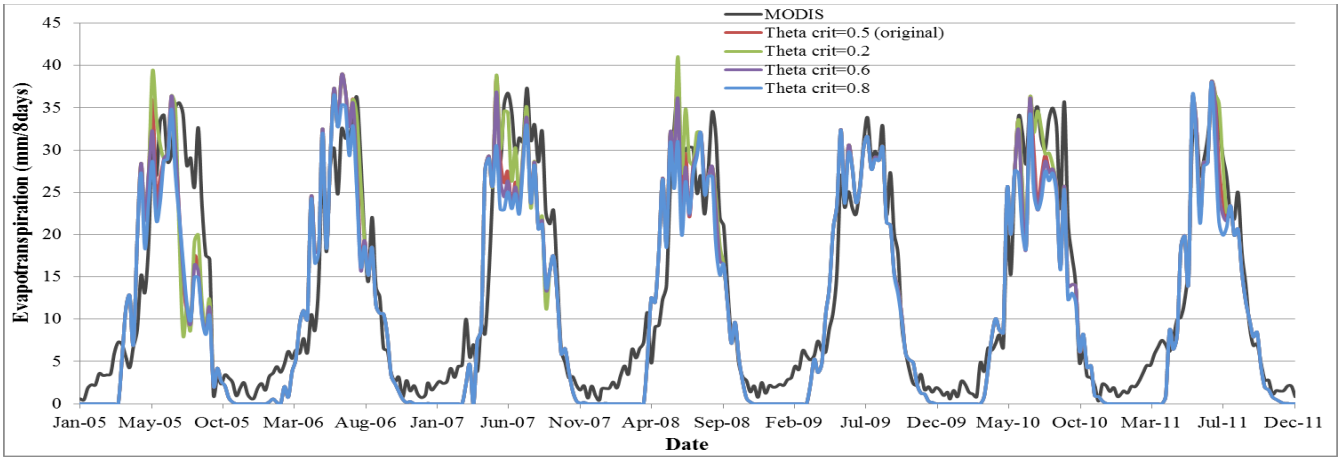

(c)

Figure 7: Model evapotranspiration time series variation under different parameter values, (a) soil water capacity, (b) PET ALPHA, (c) Theta critical

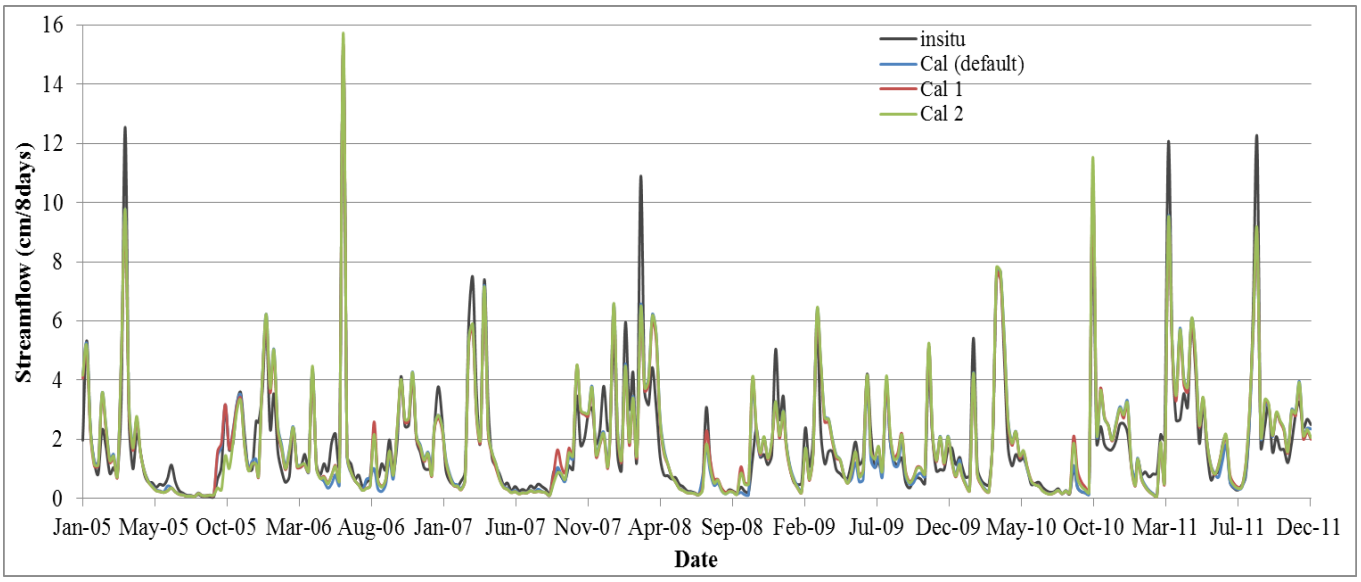

(a)

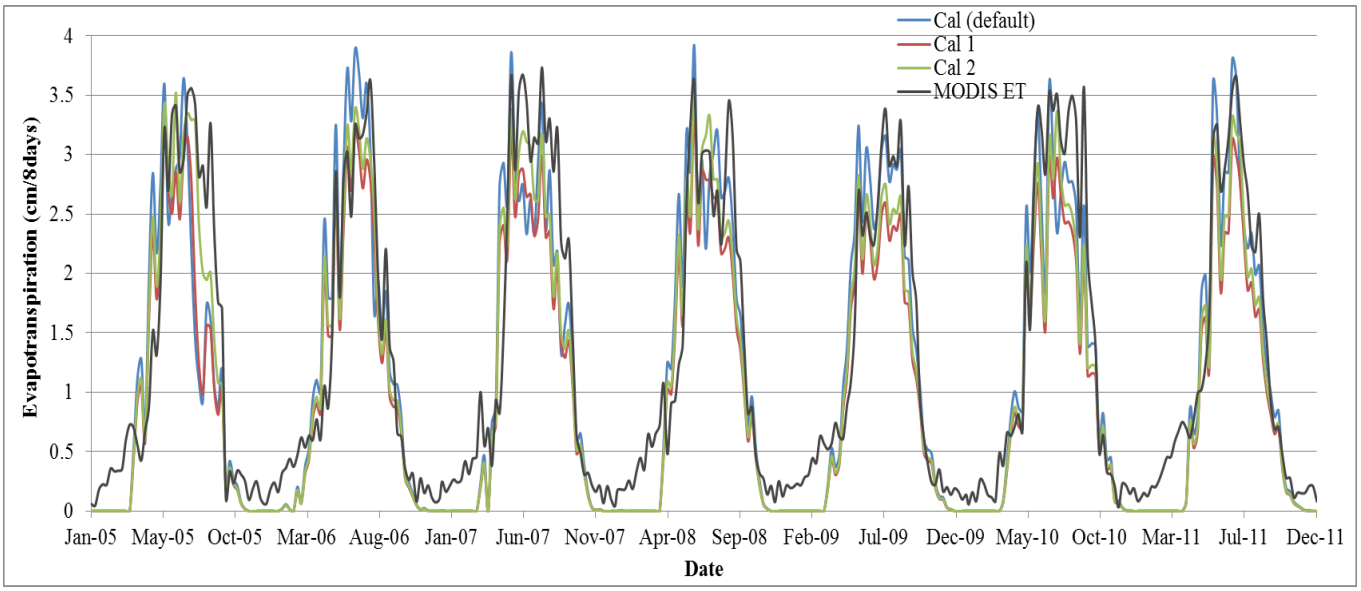

(b)

Figure 8: Streamflow (a) and evapotranspiration (b) time series variation under different calibration scenarios

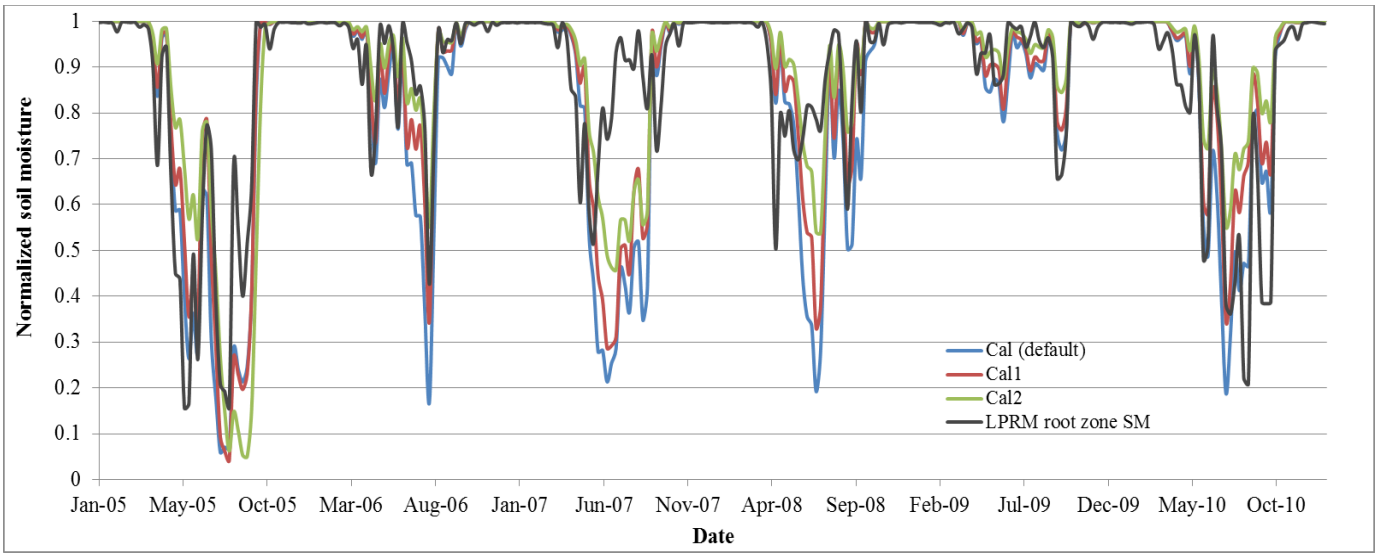

Figure 9: Comparison between estimated water content in the unsaturated zone from different calibration scenarios and the LPRM root zone soil moisture estimates (normalized and 8-day averaged)

Table 2: NS coefficient

	Calibration period		Simulation period	
	Model Q vs. in situ Q	Model ET vs. MODIS ET	Model Q vs. in situ Q	Model ET vs. MODIS ET
Default calibration	0.775	0.645	0.822	0.764
Cal 1	0.782	0.710	0.821	0.750
Cal 2	0.779	0.755	0.812	0.773
Cal 3	0.779	0.755	0.812	0.773
CalDN1	0.788	0.727	0.825	0.753
CalDN2	0.784	0.767	0.826	0.771
CalDN3	0.784	0.767	0.826	0.771

Table 3: Calibrated parameter values

Parameters	Default calibration	Cal 1	Cal 2	CalDN1	CalDN2
Precip correct factor	1.031	0.979	1.011	0.996	1.019
Melt Coeff	0.289	0.274	0.284	0.279	0.286
Smin factor	0.207	0.183	0.199	0.188	0.199
Smax factor	1.089	1.6	2.713	1.66	3.134
Runoff recess coeff	0.5	0.507	0.499	0.504	0.499
Recess coeff	0.059	0.063	0.064	0.063	0.0649
Bypass coeff	0.064	0.064	0.063	0.059	0.063
PET ALPHA	1.28 (not calibrated)	1.051	1.115	0.914	0.961
Soil water cap	10.83 cm (not calibrated)	10.83 cm (not calibrated)	29.995 cm	10.83 cm (not calibrated)	29.672 cm
Theta Crit	0.5 (not calibrated)	0.5 (not calibrated)	0.5 (not calibrated)	0.5 (not calibrated)	0.5 (not calibrated)

Table 4: Model streamflow (Q) and evapotranspiration (ET) sensitivity to temperature change

	Temperature + 1ºC		Temperature + 2ºC		Temperature + 3ºC	
	Q	ET	Q	ET	Q	ET
Default calibration	-0.0159	0.0241	-0.0302	0.0461	-0.0289	0.0433
Cal 1	-0.0156	0.0272	-0.0292	0.0517	-0.0278	0.0479
Cal 2	-0.0200	0.0329	-0.0386	0.0642	-0.0379	0.0609
CalDN1	-0.0176	0.0293	-0.0333	0.0560	-0.0317	0.0517
CalDN2	-0.0210	0.0329	-0.0405	0.0639	-0.0398	0.0607